Excitation spectra of a ^{3}He impurity on ^{4}He clusters

S. Fantoni and R. Guardiola*
SISSA and INFM DEMOCRITOS National Simulation Center, Via Beirut 2-4, I-34014 Trieste, Italy

J. Navarro
IFIC (CSIC-Universidad de Valencia), Apartado Postal 22085, E-46071-Valencia, Spain

(Dated: July 30, 2013)

The diffusion Monte Carlo technique is used to calculate and analyze the excitation spectrum of a single ^{3}He atom bound to a cluster with N ^{4}He atoms, with the aim of establishing the most adequate filling ordering of single-fermion orbits to the mixed clusters with a large number of ^{3}He atoms. The resulting ordering looks like the rotational spectrum of a diatomic molecule, being classified only by the angular momentum of the level, although vibrational-like excitations appear at higher energies for sufficiently large N.

PACS numbers: 36.40.-c 61.46.+w

I. INTRODUCTION

The study of isotopic ^{4}He-^{3}He mixed clusters is attracting a growing interest in recent years. From the experimental viewpoint, the diffraction of clusters from a transmission grating [1] has opened new perspectives in the detection and identification of small clusters. There is no evidence for the existence of the dimer ^{4}He^{3}He, but clusters $^4\mathrm{He}_N{}^3$He with $N = 2, 3, 4$ have been definitely detected [2]. It seems possible at present to resolve clearly the clusters of mass up to about 25 amu [3]. As the weakly van der Waals He-He interaction is isotope independent, the properties of such mixed clusters are determined solely by quantal effects, namely the different zero-point motion and the different statistics of the two isotopes. It turns out that helium clusters are weakly bound systems, and the lighter ones are challenging for microscopic theoretical methods.

The stability of small mixed clusters has been the object of several recent microscopic studies. Guardiola and Navarro have investigated clusters containing up to eight ^{4}He atoms and up to 20 ^{3}He atoms, based on both a Variational Monte Carlo (VMC) wave function [4, 5] and the diffusion Monte Carlo (DMC) method [6] in the fixed-node approximation. Bressanini and collaborators [7, 8, 9] have considered clusters with up to 17 ^{4}He and up to three ^{3}He atoms, by means of the DMC method, also in the fixed node approximation.

The DMC description is based in an importance sampling wave function which plays a triple role: it controls the variance of the ground-state energy, it carries on the quantum numbers and other properties of the considered cluster, and it specifies the nodal (or set of nodal) surfaces. In particular, in Refs. [4, 5, 6] the antisymmetry required for fermions has been taken into account by means of two Slater determinants, one for each spin orientation, which have been built up in terms of harmonic polynomials in the Cartesian coordinates of each fermion. Moreover, a harmonic-oscillator (HO) ordering of the fermionic shells has been assumed. Although this seems a reasonable hypothesis, supported by the findings of density-functional calculations in medium sized mixed droplets [10], from a microscopic point of view there are no conclusive *a priori* arguments in favor of such an ordering. For instance, to describe mixed systems with three ^{3}He atoms, a configuration with total angular momentum $L = 0$ has been assumed in Refs. [8, 9], which corresponds to the filling of the single-particle levels $1s^2 2s$. In contrast, the $1s^2 1p$ HO ordering, which has been assumed in Refs. [4, 5, 6], results in an angular momentum $L = 1$. The comparison of respective binding energies indicates that the $L = 1$ state has a lower energy than the $L = 0$ one. In conclusion, a more general criterion to select the shell ordering needs to be specified.

The aim of this paper is to determine the excitation spectrum of a single ^{3}He atom bound to a $^4\mathrm{He}_N$ cluster. The ordering of these single-particle levels will be relevant to describe mixed clusters with a higher number of ^{3}He atoms. It is also worth noticing that the knowledge of the one-fermion spectra in terms of the number of bosons is also relevant to determine the constants entering the rate equations which establish the formation chemical process [11], and thus the abundances in the production experiments. Our calculations are based in the DMC method, using an importance sampling wave function which carries out the orbital angular momentum of the ^{3}He relative to the $^4\mathrm{He}_N$ cluster. The DMC procedure is thus adapted so as to determine the lowest energy state of the subspace of orbital angular momentum L. In order to obtain the excited states within each subspace of angular momentum L we use an optimized form of the upper bounds provided by the sum rules method.

The paper is organized as follows. In Section II we briefly review previous investigations of $^4\mathrm{He}_N{}^3$He clusters. In Section III we present a detailed description of the method used to study the ground and excited states of these clusters. Our results are presented and discussed

*On leave of absence from Departamento de Física Atómica y Nuclear, Facultad de Física, E-46100-Burjassot, Spain

in Section IV. Some final comments are given in Section V.

II. A SURVEY OF PREVIOUS RESULTS ON ^{4}HE$_N$^{3}HE CLUSTERS

A pure $^4\mathrm{He}_{N+1}$ cluster is described by the Hamiltonian

$$H = -\frac{\hbar^2}{2m_4}\sum_{i=1}^{N+1}\nabla_i^2 + \sum_{i<j}^{N+1} V(r_{ij})\,, \qquad (1)$$

where m_4 is the mass of ^{4}He, and $V(r)$ is the interaction potential. Recent forms [13, 14, 15] of this interaction are quite similar and we will use along the paper the one known as HFD-B [13] potential.

Given that the He-He interaction is a consequence of the interaction between the electrons in the atoms, it is independent of the mass or the spin of the nucleus. To convert the $(N+1)$-th atom into an ^{3}He atom, thus dealing with the cluster $^4\mathrm{He}_N\,^3$He, corresponds to a simple change in the Hamiltonian

$$H = -\frac{\hbar^2}{2m_4}\sum_{i=1}^{N}\nabla_i^2 - \frac{\hbar^2}{2m_3}\nabla_{N+1}^2 + \sum_{i<j}^{N+1} V(r_{ij})\,, \qquad (2)$$

where m_3 is the mass of ^{3}He. The corresponding many-body problem is then not much different from that of a pure ^{4}He cluster. In the rest of the paper we will use the subindex F instead of $N+1$, to alleviate the notation.

Mixed $^4\mathrm{He}_N{}^3$He clusters containing a single fermion have been investigated using several theoretical methods. The first systematic study of the excitation spectrum of the ^{3}He atom was made by Dalfovo [16], based on a zero-range density functional. The use of a non-local finite-range density functional [10] results in small quantitative differences, related to the fact that finite-range functionals are more repulsive than zero-range ones. As the size on the drop increases, the ^{3}He atom is pushed to the surface region, due to its large zero-point motion, and for large enough clusters, the centrifugal term $L(L+1)/r^2$ entering the Schrödinger equation for the ^{3}He atom can be treated as a perturbation. Actually [12], the general trend of the spectrum is a series of tight rotational bands on top of radial excitations, related to the number of nodes in the radial wave function. In the limit of very large N, the spectrum of the ^{3}He atom becomes independent of the quantum angular momentum, forming the analogous of the two-dimensional Andreev states in bulk helium.

The so-called Lekner approximation was used in Ref. [17], where a VMC calculation was performed, as well as in Ref. [18], based on the Hypernetted-Chain method in its optimized version. Such approximation, used by Lekner [19] to analyze the Andreev states in bulk liquid, assumes that the pair correlations between ^{3}He and ^{4}He atoms are the same as those between pairs of ^{4}He atoms, so that the cluster $^4\mathrm{He}_N{}^3$He can be considered as a perturbation of the cluster $^4\mathrm{He}_{N+1}$, the perturbation being given by

$$H_I = \left(\frac{\hbar^2}{2m_4} - \frac{\hbar^2}{2m_3}\right)\nabla_F^2\,. \qquad (3)$$

Further elaboration of the perturbation scheme results in a single-particle Schrödinger equation describing the ^{3}He atom with an effective potential given by

$$V_3(r) = \left(\frac{m_4}{m_3} - 1\right)\tau_4(r) + \frac{\hbar^2}{2m_3}\frac{\nabla^2\sqrt{\rho_4(r)}}{\sqrt{\rho_4(r)}}\,, \qquad (4)$$

where $\rho_4(r)$ and $\tau_4(r)$ are respectively the ^{4}He particle and kinetic energy densities, both defined in the unperturbed system with $N+1$ bosons. Notice that the Laplacian operator acting on the square root of ρ_4 produces a strongly attractive force peaked at the surface of the cluster.

In order to classify the resulting spectra, Krotscheck and Zillich [18] defined an effective wave number $k = \sqrt{L(L+1)}/R$ for each excitation characterized by the orbital angular momentum L, where R is the equivalent hard sphere radius $R = \sqrt{5/3}r_{\rm rms}$, defined in terms of the root mean square radius $r_{\rm rms}$ of the droplet. By plotting all excitation energies as a function of k for a large number of clusters, Krotscheck and Zillich found that all results fall reasonably well on a universal quadratic line, in nice agreement with the density-functional results.

Both sets of results may be approximately pictured as molecular rigid rotor, in which the $^4\mathrm{He}_N\,^3$He cluster is viewed as a two body system, the cluster formed by the N bosons plus the single fermion, tied by a spring with a rather large rigidity constant. Various angular momentum L states are associated to each vibrational-like state of the spring, obeying the law

$$\delta E_L \approx \hbar^2 L(L+1)/2\mathcal{I} \equiv KL(L+1). \qquad (5)$$

This equation defines the rotational constant K (units of energy) in terms of the momentum of inertia $\mathcal{I}$, the later being proportional to R^2, where R is the average distance of the fermion to the center-of-mass of the bosonic cluster.

In the case of light clusters ($N < 40$) the calculations of Ref. [18] find appreciable deviations from the universal behavior Eq. (5). Small $^4\mathrm{He}_N{}^3$He clusters have been studied in Ref. [7] based on the DMC method, and in Refs. [4, 5, 6] without the use of the Lekner approximation. To this respect it is worth stressing that the Lekner approximation is basically a *weak coupling* description of the interaction of a ^{3}He atom with a ^{4}He cluster, because it does not include the perturbation that the outer ^{3}He atom should generate on the binding cluster. One may expect this picture to be satisfactory for large bosonic clusters, but inappropriate for small N. As a consequence, the interesting area to explore corresponds to the case of a small ^{4}He cluster, which may be appreciably modified by the ^{3}He atom.

III. GROUND AND EXCITED STATES DESCRIPTION

To carry out the Diffusion Monte Carlo calculation requires an importance sampling or guiding wave function, which incorporates as much as possible the characteristics of the system to be described. In particular, due to the strong short-range repulsion of the atom-atom interaction, it is advisable to introduce at least two-body Jastrow correlations. Moreover, the guiding wave function must confine the system and, finally, it has to include the bosonic symmetry related to the ^{4}He atoms and the desired quantum numbers for the ^{3}He atom. In this Section we shall describe a variational wave function which will be used to calculate the lowest-energy states for a given value of the angular momentum L of the system. Excited states corresponding to radial excitations will be estimated by means of sume-rule techniques.

A. Ground state and angular momentum excitations

In order to describe the system $^4\mathrm{He}_N{}^3\mathrm{He}$ in a state where the ^{3}He atom is in an orbital angular momentum L with respect to the $^4\mathrm{He}_N$ system, a simple but nevertheless complete wave function is given by

$$\begin{aligned}\Psi(\mathbf{r}_1,\ldots,\mathbf{r}_N,\mathbf{r}_F) &= \Phi_B(\mathbf{r}_1,\ldots,\mathbf{r}_N) \\ &\quad \Phi_M(\mathbf{r}_1,\ldots,\mathbf{r}_N,\mathbf{r}_F)\Phi_L(\mathbf{r}_F-\mathbf{R}_B)\,,\end{aligned} \tag{6}$$

where the subindexes B and F stand for bosons and fermions, respectively, whereas M refers to the mixed boson-fermion part of the wave function. The bosonic coordinates run from 1 to N and the coordinate of the fermion is labelled by F. Finally, $\mathbf{R}_B$ represents the center-of-mass coordinate of the bosonic subsystem. This model wave function includes an internal bosonic part (Φ_B) and the coupling of the fermion to individual bosons (Φ_M) as well as to the bosonic cluster (Φ_L).

We have taken Φ_B and Φ_M to be of the Jastrow form

$$\Phi_B(\mathbf{r}_1\ldots\mathbf{r}_N) = \prod_{i<j=1}^{N} \mathrm{e}^{f_B(r_{ij})} \tag{7}$$

$$\Phi_M(\mathbf{r}_1\ldots\mathbf{r}_N,\mathbf{r}_F) = \prod_{i=1}^{N} \mathrm{e}^{f_M(r_{iF})}\,, \tag{8}$$

with

$$f_{B,M}(r) = -\frac{1}{2}\left(\frac{b_{B,M}}{r}\right)^{\nu} - p_{B,M}\,r\,. \tag{9}$$

The two-body correlation terms include a short-range part, associated with the parameters b_B and b_M, and a long-range confining part associated with the parameters p_B and p_M. The short-range part is mainly related to the small-distance behavior of the relative two-body wave function. Consequently, the parameters $b_{B,M}$ and ν have been taken to be the same for all systems studied, and in our calculations they have been kept fixed to the values $b_B = 2.95$ Å, $b_M = 2.90$ Å and $\nu = 5.2$, as obtained in our previous calculations for pure ^{4}He and ^{3}He clusters [20, 21, 22], by direct minimization of the expectation value of the energy. On the other hand, the long-range confining parameters $p_{B,M}$ have been determined by means of the VMC method.

In the absence of the last term Φ_L of the importance sampling wave function (6) we would describe a state of null angular momentum, explicitly translational invariant and including the bosonic symmetry of the indistinguishable ^{4}He atoms. The role of the last term Φ_L of Eq. (6), describing the motion of the fermion, is to determine the value of the orbital angular momentum L. It has been taken as a long-range wave function depending on the relative coordinate of the fermion with respect to the center-of-mass of the bosons, $\mathbf{r} = \mathbf{r}_F - \mathbf{R}_B$. The explicit form used is the harmonic polynomial

$$\Phi_L(\mathbf{r}) = r^L P_L(\cos\theta_r)\,. \tag{10}$$

This function is particularly simple and corresponds to a state with orbital angular momentum L and null third component. One could have taken a more sophisticated form, by putting a radial dependence different from the simple r^L, but it is reasonable to expect the DMC algorithm to be able to improve this simple and computationally convenient form. By making this part of the trial wave function to depend on the relative distance of the fermion to the center-of-mass of the bosons the translational invariance of the importance sampling wave function is not spoiled. Notice that if we had considered the function to depend on the distance of the fermion to the center-of-mass of the full system, the only difference would have been a trivial scale factor.

With the structure of the importance sampling wave functions one may describe the lowest-energy states for each angular momentum L. It should be mentioned that apart from the case $L = 0$ for which $\Phi_L = 1$, all other cases correspond to functions with a nodal surface, with nodes depending only on the angular variables. This fact has to be taken into account when using the DMC algorithm.

B. Radial excitations

When considering a subspace of angular momentum L the DMC algorithm gives only the energy of the ground state of that subspace, and there is no information about the excited states of the same angular momentum. A way to have an estimate, actually an upper bound, of the first excited state is to use the sum rules method [23].

Consider the exact ground state for a given angular momentum L, represented here by Ψ_{0L}, and the full set of eigenstates of this subspace ordered by increasing energy and represented by $\{\Psi_{nL}, E_{n,L}\}, n = 0, 1\ldots$. Let $Q(\mathbf{R})$

be an arbitrary Hermitian operator which may depend on all atomic coordinates, which is assumed to be scalar under rotations, i.e., to commute with **L** and **S**. Let us consider the sum rule of order p

$$M_L^{(p)}[Q] = \sum_{(n,\ell)\neq(0,L)} (E_{n\ell} - E_{0L})^p |\langle \Psi_{n\ell}|Q|\Psi_{0L}\rangle|^2 \,, \quad (11)$$

where the sum extends to all eigenstates of the Hamiltonian but the lowest energy state of angular momentum L. This is important because in order to obtain easily computable properties it will convenient to use the completeness relation. Because of the assumed properties of Q only states with angular momentum $\ell = L$ will contribute to the sum. The $p = 1$ rule fulfills the property

$$\begin{aligned} M_L^{(1)}[Q] &\equiv \sum_{n\neq 0} (E_{nL} - E_{0L}) |\langle \Psi_{nL}|Q|\Psi_{0L}\rangle|^2 \\ &\geq (E_{1L} - E_{0L}) M_L^{(0)}[Q] \,, \end{aligned} \quad (12)$$

from which one obtains an upper bound to the energy of the first excited state of the subspace L

$$E_{1L} - E_{0L} \leq \frac{M_L^{(1)}[Q]}{M_L^{(0)}[Q]} \,. \quad (13)$$

The evaluation of the sum rules is simpler than seem, because of the relations

$$M_L^{(0)}[Q] = \langle \Psi_{0L}|Q^2|\Psi_{0L}\rangle - |\langle \Psi_{0L}|Q|\Psi_{0L}\rangle|^2 \quad (14)$$

$$M_L^{(1)}[Q] = \frac{1}{2}\langle \Psi_{0L}|[Q,[H,Q]]|\Psi_{0L}\rangle \,. \quad (15)$$

The double commutator may be simplified for a general Hamiltonian of the form given in Eq. (2), obtaining

$$\begin{aligned} M_L^{(1)} &= \frac{\hbar^2}{2m_4}\langle \Psi_{0L}| \sum_{i=1}^{N} |\nabla_i Q|^2 |\Psi_{0L}\rangle \\ &+ \frac{\hbar^2}{2m_3}\langle \Psi_{0L}||\nabla_F Q|^2|\Psi_{0L}\rangle \,. \end{aligned} \quad (16)$$

Note that to compute these expressions one only requires knowledge of the ground state wave function of the angular momentum L subspace.

This method was used in Ref. [23] to obtain upper bounds to the first $L = 0$ excitation, as well as to the low-lying even-L states. Given that we are obtaining the $L \neq 0$ excitations directly from the DMC procedure, the sum rules method will be used here to obtain the energies of the first excited states in each L-subspace. In the Appendix we use the sum rule method to also estimate $L \neq 0$ excitations based in the knowledge of Ψ_{00} by relaxing the scalar character of Q as an alternative to the direct DMC calculations.

The upper bound given by Eq. (13) is a functional of the operator Q, so it may be variationally optimized by equating to zero its functional derivative with respect to Q. Unrestricted minimization will give rise to the unpractical relation $Q|\Psi_{0L}\rangle = |\Psi_{1L}\rangle$, its solution being equivalent to the solution of the many-body Schrödinger equation for the excited state. An alternative is to optimize the operator inside a restricted subspace, which is the approach followed by Chin and Krotscheck [24, 25] and is closely related to the procedure of Krisna and Whaley [26].

Here we have followed a simpler procedure, based in the linear expansion of the operator in a basis of easily computable operators. To determine the basis we have assumed a single-particle-like form for the operator, by considering that it depends only on $\mathbf{r}_F - \mathbf{R}_B$, i.e., on the coordinate of the fermion referred to the bosonic center-of-mass

$$Q = Q(\mathbf{r}_F - \mathbf{R}_B). \quad (17)$$

This simple form preserves the translational invariance and does not spoil the boson symmetry of the ^{4}He subsystem. For this type of general operator Eq. (16) can be further simplified, since the following relation

$$\nabla_i Q(\mathbf{r}_F - \mathbf{R}_B) = -\frac{1}{N}\nabla_F Q(\mathbf{r}_F - \mathbf{R}_B)$$

holds. The resulting sum rule M_1 becomes

$$M_1 = \frac{\hbar^2}{2\mu}\langle \Psi_{0L}| \, |\nabla_F Q|^2 |\Psi_{0L}\rangle \,, \quad (18)$$

where $\mu = (Nm_4m_3)/(Nm_4 + m_3)$ is the reduced mass of the ^{3}He atom and the ^{4}He cluster.

In the calculations to be described below the monopole operator has been optimized by using a simple functional form depending on few parameters,

$$Q(\mathbf{r}_F - \mathbf{R}_B) = \sum_{m=1}^{5} C_m q_m(\mathbf{r}_F - \mathbf{R}_B) \,, \quad (19)$$

with

$$q_m(\mathbf{R}) = |\mathbf{r}_F - \mathbf{R}_B|^m \,. \quad (20)$$

The minimization of the upper bound of Eq. (13) with respect to C_m, for angular momentum L, gives rise to a generalized eigenvalue problem,

$$\mathcal{M}^{(1)}_{mn} C_n = \mathcal{E}\mathcal{M}^{(0)}_{mn} C_n \,, \quad (21)$$

with a Hamiltonian-like matrix

$$\mathcal{M}^{1}_{mn} = \frac{\hbar^2}{2\mu}\langle \Psi_{0L}|\nabla_F q_m \nabla_F q_n|\Psi_{0L}\rangle \quad (22)$$

and a normalization matrix

$$\begin{aligned} \mathcal{M}^{0}_{mn} &= \langle \Psi_{0L}|q_m q_n|\Psi_{0L}\rangle \\ &- \langle \Psi_{0L}|q_m|\Psi_{0L}\rangle\langle \Psi_{0L}|q_n|\Psi_{0L}\rangle. \end{aligned} \quad (23)$$

The lowest eigenvalue of Eq. (21) provides an optimized upper bound. By inserting Eq. (20) into Eqs. (22) and (23) the matrices are further simplified to

$$\mathcal{M}^{(1)}_{mn} = \frac{\hbar^2}{2\mu} mn \langle \Psi_{0L}| \, |\mathbf{r}_F - \mathbf{R}_B|^{m+n-2} |\Psi_{0L}\rangle \qquad (24)$$

and

$$\begin{aligned} \mathcal{M}^{(0)}_{mn} &= \langle \Psi_{0L}| \, |\mathbf{r}_F - \mathbf{R}_B|^{m+n} |\Psi_{0L}\rangle \qquad (25) \\ &- \langle \Psi_{0L}| \, |\mathbf{r}_F - \mathbf{R}_B|^{m} |\Psi_{0L}\rangle \langle \Psi_{0L}| \, |\mathbf{r}_F - \mathbf{R}_B|^{n} |\Psi_{0L}\rangle. \end{aligned}$$

It is worth keeping in mind that in our DMC calculations the matrix elements $\mathcal{M}^{(p)}_{mn}$ are based in a mixed estimate, so the strict variational character of Eq. (13) may be lost.

Some insight on the structure of these excitation may be drawn by considering the leading $m = n = 1$ terms of both the Hamiltonian and norm matrices. For this one-dimensional subspace the upper bound to the radial excitation energy is given by

$$E_{1L} - E_{0L} \leq \qquad (26)$$
$$\frac{\hbar^2}{2\mu} \frac{1}{\langle 0L| \, |\mathbf{r}_F - \mathbf{R}_B|^2 |0L\rangle - |\langle 0L| \, |\mathbf{r}_F - \mathbf{R}_B| \, |0L\rangle|^2} .$$

The size of this bound depends on the difference between the mean square radius and the squared mean radius of the fermion with respect to the boson center-of-mass. This difference will be small if the distribution of the fermion with respect to the boson center-of-mass is sharply peaked near a given value say R_0, corresponding to a rather rigid spring. Then the denominator will be small and the radial excitation will have large energy.

The excited states considered in this section result from excitations related to the distance between the fermion and the center-of-mass of the cluster of bosons. The underlying optimal wave function (not determined, however, from the DMC procedure) should have at least a node along this radial coordinate, in order to be orthogonal to the angular momentum L ground state, and may be properly termed as a *radial excitation*.

C. Computational details

The DMC algorithm [27, 28] is nowadays a well-known and used technology. It is based in integrating the imaginary-time Schrödinger equation for an auxiliary function $f(\mathbf{R}, t) = \Phi_{\rm var}(\mathbf{R})\Psi(\mathbf{R}, t)$ which is the product of a trial wave function $\Phi_{\rm var}$ and the true ground-state wave function $\Psi(\mathbf{R}, t)$. The solution is given in terms of an approximate small-time Green funtion $G(\mathbf{R}, \mathbf{R}', \tau)$

$$f(\mathbf{R}', t + \tau) = \int d\mathbf{R} G(\mathbf{R}', \mathbf{R}, \tau) f(\mathbf{R}, t) \qquad (27)$$

by means of a series of small time steps τ. We have used the $O(\tau^3)$ approximate Green function [29, 30] which provides an $O(\tau^2)$ approximation for the energy. In our calculations we have used a set of 1000 walkers, on the average, a value of $\tau = 0.0002\,\mathrm{K}^{-1}$, 8000 iterations to settle down the system and 80000 iterations to compute the averages. For $N \geq 40$ we have used a smaller time step $\tau = 0.00015\,\mathrm{K}^{-1}$ and the number of iterations has been doubled.

The wave function is not definite positive when $L \neq 0$, and this leads to the known and irritating *sign problem* of the DMC algorithm. We have used the so-called *fixed node approximation*. The auxiliary function $f(\mathbf{R}, t)$ will remain positive if both functions $\Phi_{\rm var}$ and Ψ have (at any time) the same nodal surfaces. The fixed node approximation consists in killing any walker which attempts to cross a nodal surface. It has been shown [27, 28, 31] that this procedure leads to an upper bound to the ground state.

IV. ENERGETICS OF ^{4}HE$_N$^{3}HE CLUSTERS

We have first performed a VMC calculation to determine the free parameters p_B and p_M of the importance sampling wave function. As mentioned in the previous Section, the parameters b_B, b_M and ν are fixed by the atom-atom interaction at very short distances, and do not depend on the size of the cluster. On the contrary, the long-range parameters $p_{B,M}$ are very sensitive to the number of bosons. Their values, determined by minimizing the ground state expectation value of the Hamiltonian, are reported in Table I.

TABLE I: Optimal values of the parameters (in Å^{-1}) for the variational description of the system ^{3}He^{4}He$_N$, as a function of the number of bosons N. The last two columns contain the ground state VMC and DMC energies (in K). Figures in parenthesis are the standard deviations of the Monte Carlo calculations.

N	p_B	p_M	$E_{\rm VMC}$	$E_{\rm DMC}$
5	0.1250	0.0900	−1.59(2)	−1.862(4)
10	0.0672	0.0395	−8.99(6)	−9.763(9)
15	0.0491	0.0321	−19.17(13)	−21.39(2)
20	0.0365	0.0226	−31.09(12)	−35.42(3)
25	0.0298	0.0187	−44.51(16)	−51.20(3)
30	0.0253	0.0160	−59.2(2)	−68.03(5)
35	0.0220	0.0140	−74.5(3)	−86.13(6)
40	0.0195	0.0125	−90.5(3)	−104.90(9)
45	0.0176	0.0113	−106.1(3)	−124.63(5)
50	0.0160	0.0104	−122.8(5)	−144.67(5)

One can see that the values of these parameters decrease when the number of bosons increase, as it should correspond to a drop, its size growing with the number of constituents. Notice that, for any given number of bosons, the parameter p_M, controlling the boson-fermion distance, is significantly smaller than the parameter p_B controlling the boson-boson distance. This reflects the fact that the light particle stands near the surface of the bosonic drop.

FIG. 1: Raw DMC results (boxes with error bars) and the least-squares fits. From top to bottom, the figures show the dissociation energy and the excitation energies for $L = 1 - 4$, all measured in K, as a function of the number of bosons N. The dashed line in the lower four figures is the smoothed dissociation limit.

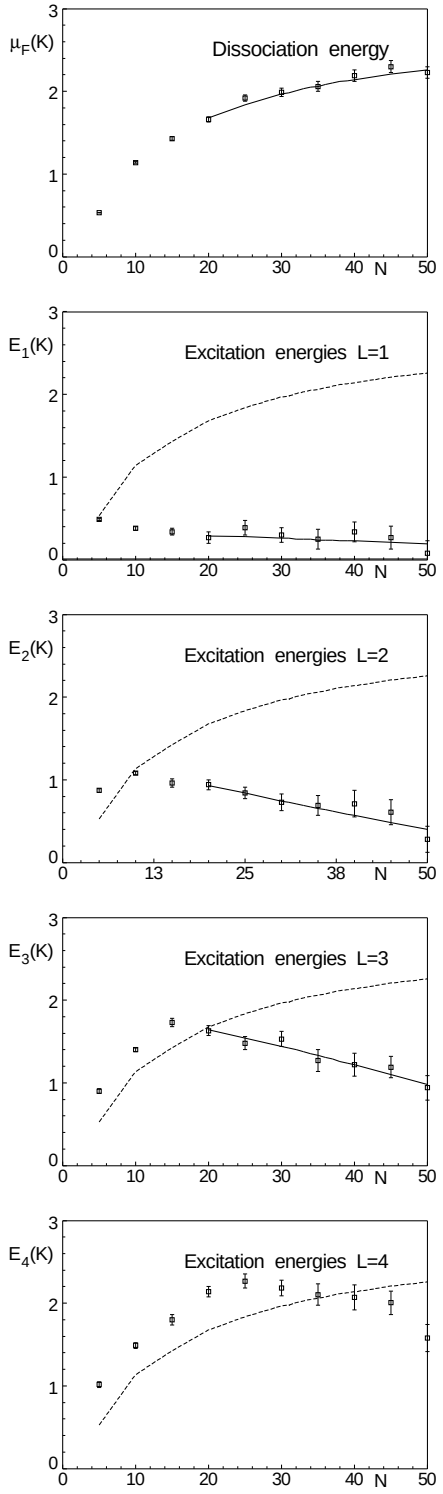

In Table I the ground state energies obtained within the VMC calculation as well as with the improved DMC method are also displayed. The later are significantly lower than the former, thus revealing that the variational trial functions are not of high quality. They could be improved by adding either medium-range terms to the two-body Jastrow correlation or three-body Jastrow correlations. Notice that improving the importance sampling wave function will not affect the DMC results of Table I except for the statistical error. Nevertheless, it could lead to better upper bounds for the $L \neq 0$ energies.

The statistical errors of the DMC energies grow steadily with the number of bosons. As a consequence, the determination of the excitation energies becomes less and less accurate for large N. The excitation energies E_L are obtained as the difference of two independent calculations, one for $L = 0$ (E_{00}) and the other for the desired value of the angular momentum (E_{0L}). These two energies have very close values, thus magnifying the statistical error of their difference. As a consequence, the direct plot of the excitation energies will show fluctuations. In order to control them we have fitted all cases between $N = 30$ and $N = 50$ with a liquid-drop like formula, i.e. a third-order polynomial fit in terms of the variable $N^{1/3}$.

The ^{3}He chemical potential, or ^{3}He dissociation energy, is defined as

$$\mu_F = E_{00}(^4\mathrm{He}_N) - E_{00}(^4\mathrm{He}_N\, ^3\mathrm{He})\,. \qquad (28)$$

It corresponds to the energy required to eject the ^{3}He atom from the mixed system in its ground state ($L = 0$). According to the definition, μ_F is a positive quantity and its value is relevant because the states whose excitation energy is above it are not bound. To control the statistical fluctuations in μ_F we have again fitted the raw differences with a liquid-drop formula. In Fig. 1 are plotted the raw DMC results for the chemical potentials and the excitation energies, as well as their respective fits as described above. For $L = 4$ there were too few points to carry out that fit, and we have only plotted the raw DMC results.

The corresponding values for bound levels are displayed in Table II for excited states with $L = 1$ to $L = 4$ and for systems with different number of bosons. The total energy of the ground state (E_{00}) has been already quoted in the last column of Table I. The excitation energies displayed in Table II are the raw DMC differences for systems with $N < 20$ and the results of the least squares fit otherwise.

The excitation energies of radially excited levels obtained with the sum rules method described above are shown in Fig. 2 for $L = 0, 1, 2$. These levels are close to the dissociation limit, above it for $N < 20$ and below afterwards, for $L = 0, 1$. The radial excitation for $L = 2$ is always above the dissociation limit, with the exception of N near 50, which signals the threshold for the binding of this level. One should keep in mind that the upper bound character of the excitation energies, as expressed by Eq. (13), is not strictly satisfied in the present calcu-

TABLE II: Excitation energies E_L, in K, of $^4He_N{}^3He$ clusters for $L = 1 - 4$ and $N = 5 - 50$ in steps of 5 atoms. The values quoted are the result of the least squares fit described above for $N \geq 20$ and raw DMC results for $N < 20$, with the exception of the $L = 4$ column which contains the raw DMC results. The last column displays the ^{3}He dissociation limit.

N	ΔE_1	ΔE_2	ΔE_3	ΔE_4	μ_F
5	0.48(1)				0.53
10	0.37(2)	1.08(2)			1.14
15	0.33(4)	0.96(5)			1.43
20	0.28	0.93	1.64		1.68
25	0.27	0.84	1.54		1.85
30	0.25	0.74	1.44	2.18(10)	1.97
35	0.23	0.65	1.33	2.10(12)	2.05
40	0.22	0.57	1.22	2.07(15)	2.14
45	0.20	0.48	1.10	2.01(14)	2.21
50	0.18	0.40	0.98	1.58(16)	2.26

FIG. 2: Radial excitations (in K) on top of $L = 0$ to $L = 2$ lowest levels. The squares are the results obtained directly from the DMC calculation, the continuous line is a guiding line for these excitations and the dashed line is the dissociation limit.

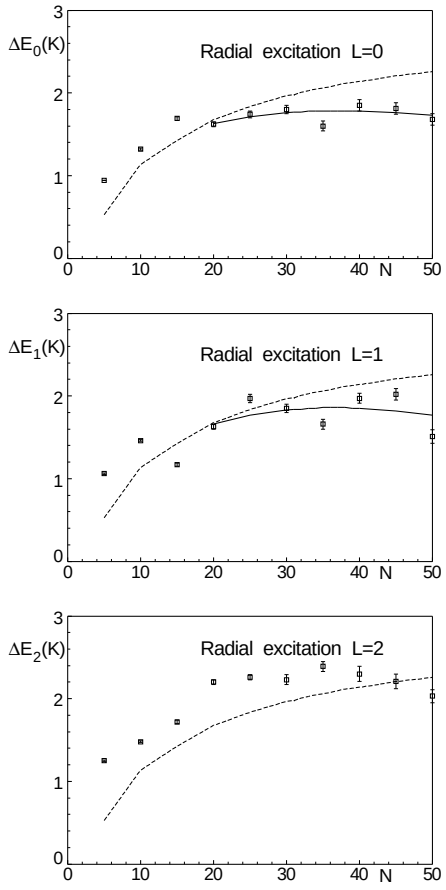

lations because the radial excitation energies have been computed by means of (approximate) mixed matrix elements; therefore, some of the referred levels may not be bound in reality. For $L > 2$ the radial excitations are clearly unbound up to $N = 50$.

The bound level spectra resulting from our calculations are collected up in Fig. 3. The bound levels are grouped by the value L of the angular momentum, indicated in the right side of the figure, with the symbol 0^* signaling the radial excitations of the ground state.

FIG. 3: Excitation energies of the ^{3}He bound excited levels in a mixed droplet as a function of the number of ^{4}He atoms. The levels are ordered by the value L of the angular momentum, written in the right side. Index 0^* refers to the to the radial excitations of the ground state and corresponds in the figure to dashed lines. The dotted line is a guiding line joining the chemical potential μ_F.

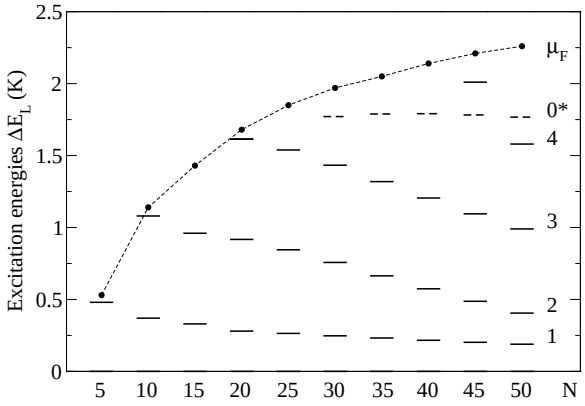

As we have mentioned in Section II, one could expect these spectra to look like a series of rotational bands, with the excitation energies roughly proportional to the value $L(L+1)$, where L is the angular momentum of the excited level. That is to say that the quantities

$$K = \frac{E_{0L} - E_{00}}{L(L+1)}\,, L \neq 0\,, \tag{29}$$

which correspond to the rotational constants (*cf.* Eq. 5), should be expected to depend only on N, and not on the angular momentum L. This is indeed the case, as shown in Table III. The values of the rotational constants smoothly decreases as N increases, as expected because of the dominant dependence on $\langle 1/|\mathbf{r}_F - \mathbf{R}_B|^2\rangle$.

V. STRUCTURE OF $^4HE_N{}^3HE$ CLUSTERS

A complementary information about the nature of the excitations is provided by the density distributions of the fermion with respect to the center-of-mass of the system. Given that we are dealing with non-zero angular momentum states, to simplify the presentations we show them in Figure 4, for the bound states of systems with $N = 10$, 20, 30, and 40. No plot of radially excited states is given,

TABLE III: Rotational constants, in K, as defined in Eq. (29), for the bound levels with $L = 1 - 4$.

N	$L=1$	2	3	4
5	0.24			
10	0.19	0.18		
15	0.17	0.16		
20	0.14	0.16	0.14	
25	0.14	0.14	0.13	
30	0.13	0.12	0.12	
35	0.12	0.11	0.11	0.11
40	0.11	0.10	0.10	0.10
45	0.10	0.08	0.09	0.10
50	0.09	0.07	0.08	0.08

because the calculation of excitation energies using sum rules does not allow to obtain the density distributions. In all the figures ρ_B corresponds to the boson distribution of the ground state with $L = 0$, as there are no appreciable differences between the boson distributions for drops in other L-excited state. This fact supports the model of an ^{3}He atom in a potential well created by the $^4\mathrm{He}_N$ atoms, like in the Lekner approximation.

Table IV lists the values of the root mean square radii of bosons and fermions with respect to the center of mass. Only the ground state boson radius has been displayed in this table since it is almost independent of the angular momentum L. The boson radius grows monotonically with the number of bosons, following a rough $N^{1/3}$ law, as could be expected. The fermion radii are given for the states with angular momentum from $L = 0 - 4$. At fixed L, the fermion radii increases smoothly with N, except for the lowest value signaling the threshold of stability. In that case, the fermion radius may be abnormally large, indicating that the system is only slightly bound. A flashy case is $N = 30, L = 4$ due to its very large fermion radius. This level is almost surely unbound and the DMC algorithm ejects the fermion far away from the center-of-mass of the drop; eventually the ^{3}He will move to infinity if the random walk were long enough.

TABLE IV: Average boson (second column) and fermion (third to seventh columns) distances (in Å) to the center-of-mass of the cluster. Empty entries correspond to unbound systems.

N	r_B	$L=0$	$L=1$	$L=2$	$L=3$	$L=4$
5	4.67	6.16	8.04			
10	5.16	6.79	7.87	10.45		
15	5.49	7.01	8.02	8.93	10.74	
20	5.86	7.50	8.12	9.19	10.25	
25	6.15	7.80	8.42	9.26	10.07	
30	6.41	8.32	9.09	9.67	10.67	17.88
35	6.64	8.50	9.14	9.87	10.41	11.62
40	6.85	8.79	9.37	9.90	10.85	11.79
45	7.05	9.02	9.68	10.18	10.79	11.78
50	7.24	9.17	9.81	10.47	11.08	12.00

The picture which emerges from the densities plot in Fig. 4 and from the values of radii in Table IV is the expected one. The fermion is always located at the surface of the boson cluster, and increasing the value of the angular momentum produces the fermion to go away from the boson cluster.

FIG. 4: The angular-averaged density distributions of the fermion with respect to the center-of-mass of the system $^4\mathrm{He}_N$ ^{3}He for several values of the number of bosons N and the fermionic orbital angular momentum L. The boson density distribution with respect to the center-of-mass appearing in the plot has been arbitrarily divided by 20 to appreciate the fermion distributions in the figures.

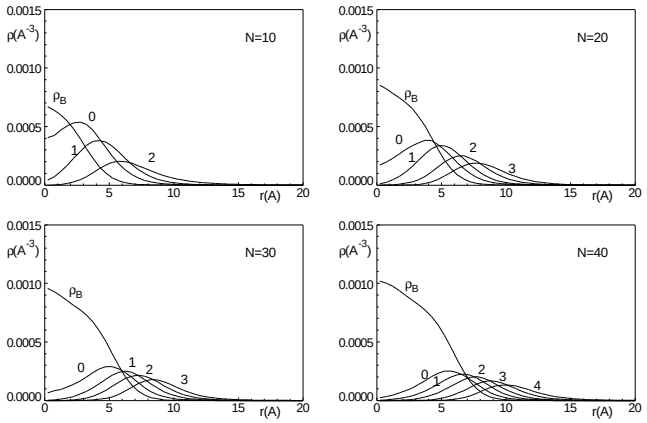

To ascertain the goodness of Lekner approximation we have plotted in Fig. 5 the boson distributions corresponding to two pure ^{4}He system with N and $N + 1$ together with the boson distribution for N bosons plus one fermion. The distributions corresponding to $N = 40$ are almost superimposed, thus revealing the rigidity of the bosonic core in front of the addition of a fermion. On the other hand, there are sizable differences between the three distributions for $N = 10$, revealing the effect of the dopant on the bosonic cluster. In other words, there is a weak coupling regime (Lekner approximation) for large N but a strong coupling regime for light drops.

VI. CONCLUSIONS

We have permormed DMC simulations, in conjunction with the sum rule method of Ref. [23], to compute the excitation spectrum of a ^{3}He impurity in ^{4}He clusters. The rotational levels, namely the lowest energy levels within each angular momentum L subspace have been computed by including in the guiding function a term $\Phi_L(\mathbf{r}_F - \mathbf{R}_B)$, generating an eigenfunction with good angular momentum quantum numbers. On the other hand, the radial excitations have been estimated by computing an optimized upper bound obtained with the sum rules of order 0 and 1.

Important results have been obtained for the shell ordering of the ^{3}He orbitals. First of all, the excitation spectrum contains a limited set of bound excited levels, whose number increases with the number N of bosons.

FIG. 5: Comparison of the boson distributions in Å^{-3}, normalized to the number of particles, for the pure bosonic systems with N and $N+1$ and the mixed drop with N bosons and one fermion. Two cases are shown, $N=10$ and $N=40$. Labels 10 and 11 refer to pure bosonic systems, and $10+1$ to the doped drop. In the case of $N=40$ the curves are almost indistinguishable.

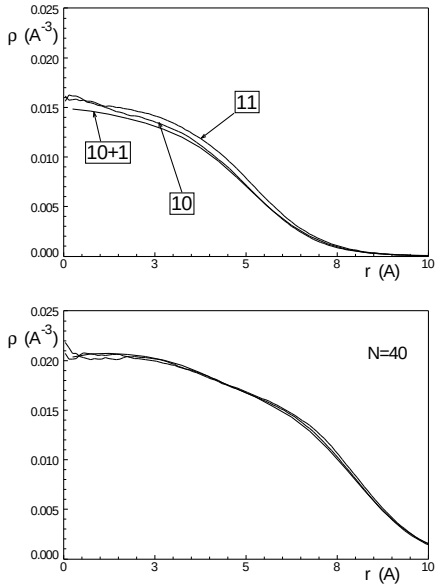

Indicating the n-th radial excitation of the state with angular momentum L with notation $(n+1)L$, using the usual spectroscopic letters for the values of L, we find the excitation energies to follow a rotational spectrum, thus suggesting a shell ordering of levels $1s\,1p\,1d\,1f\,1g\ldots$. Starting at $N\approx 20$, the $2s$ radial excited state appears as an *intruder* within the rotational band. Presumably, at a larger value of N, the $2p$ radial excitation will appear, an so on. The obtained level ordering is different from both the $1s\,1p\,1d\,2s\,1f\,2p\ldots$ of the three-dimensional harmonic oscillator and the $1s\,2s\,1p\,3s\,2p\ldots$ typical of atoms.

This ordering of levels should be taken into account specially when dealing with mixed drops with a number of bosons much larger than the number of fermions. Note however that whereas the DMC algorithm is able to improve the quality of the model or importance sampling wave function as far as the bosonic correlations are concerned, with respect to the fermionic part it will maintain the structure of the nodal surfaces. There remains however an important question, namely the relevance of these results for pure fermionic systems or for mixtures with a comparable number of bosons and fermions. The fermions are expected to play a double role: on the one side, fermions are creating some kind of self-consistent central field, analogously to the bosons, and on the other side they are subject to the Pauli principle effects. So, in a first approximation, one may assume that the level ordering of such systems is close to that of the system $^3\text{He}\,^4\text{He}_{N_4+N_3-1}$. However, one should not discard the analysis of other alternatives. On the basis of our results it becomes clear that previous microscopic calculations of pure fermionic drops as well as of mixed drops should be reconsidered, by using an improved importance sampling wave function based on realistic shell orderings.

Acknowledgments

This work has been supported by MCyT/FEDER (Spain), grant number BMF2001-0262, GV (Spain), grant number GV01-216 and MIUR (Italy), cofin-2001025498. One of us (RG) acknowledges financial support of the Secretaría de Estado de Educación y Universidades (Spain), Ref. PR2003-0374, as well as DEMOCRITOS by his hospitality.

APPENDIX A: THE SUM RULES METHOD APPLIED TO EXCITATIONS OF ANGULAR MOMENTUM L

We have described above the use of the moment method to compute the radial excitation energies. The method may be also used to determine upper bounds to the excitation energies of states with angular momentum L, as we shall show in this Appendix. The resulting information will complement the one obtained directly by the DMC method, and is particularly relevant for the cases $L=1,2$ where the direct calculation of the excitation energies is affected by a rather large relative error, being the difference of two large quantities, specially for large values of N.

To obtain upper bounds to the excitation energy of a state of angular momentum $L\neq 0$ it is convenient to use for the operator Q a form which behaves as an angular momentum tensor of rank L. A simple way is to consider the value

$$Q^{(L)}(R)=f(|\mathbf{r}_F-\mathbf{R}_B|)(x_F+iy_F-X_B-iY_B)^L\,. \quad \text{(A1)}$$

For the function f we have considered a power expansion

$$f(r)=\sum_{n=0} C_n r^n\,, \quad \text{(A2)}$$

with parameters C_n to be determined after optimization of the upper bound. To fulfill the requirements which lead to Eq. (13) we should consider the Hermitian part of this operator. In fact, as we are interested in excitations of angular momentum L, irrespective of the value of the projection of angular momentum along some fixed axis, a linear combination like

$$\tilde{Q}^{(L)}=\left(Q^{(L)}+{Q^{(L)}}^\dagger\right)/\sqrt{2}$$

will be adequate. This combination has the advantadge that sum rules M_0 and M_1 are expressed by Eqs. (14)

TABLE V: Upper bounds to the excitation energy of the lowest energy state for L=1 to 4

N	E_1	E_2	E_3	E_4	μ_F
10	0.43	1.01	1.57	2.04	1.14
15	0.41	1.03	1.75	2.45	1.43
20	0.36	0.92	1.59	2.27	1.68
25	0.33	0.87	1.55	2.31	1.85
30	0.28	0.77	1.41	2.17	1.97
35	0.28	0.74	1.34	2.06	2.05
40	0.25	0.69	1.29	2.06	2.14
45	0.24	0.66	1.24	1.97	2.21
50	0.23	0.64	1.20	1.92	2.26

and (16), replacing operator Q in these expressions with either $Q^{(L)}$ or its Hermitian conjugate $Q^{(L)\dagger}$.

As in the case of radial excitations, we end up with a generalized eigenvalue problem, the required matrix elements of the moment operators being given by

$$\mathcal{M}^1_{mn} = \frac{\hbar^2}{2\mu}\langle 0|\nabla[r^m(x-iy)^L]\cdot\nabla[r^n(x+iy)^L]|0\rangle \quad \text{(A3)}$$

and

$$\mathcal{M}^0_{mn} = \langle 0|r^{m+n}(x^2+y^2)^L|0\rangle\,, \quad \text{(A4)}$$

with $\mathbf{r} = \mathbf{r}_F - \mathbf{R}_B$. Notice that $< 0|Q^{(L)}|0 >= 0$.

As the expectation values are taken with respect to the $L = 0$ ground state, one may take the angular averages of the operators. After some algebra there results

$$\mathcal{M}^0_{mn} = \langle 0|r^{2L+m+n}|0\rangle \mathcal{I}_L \quad \text{(A5)}$$

and

$$\mathcal{M}^1_{mn} = \frac{\hbar^2}{2\mu}\langle 0|r^{2L+m+n-2}|0\rangle[2L^2\mathcal{I}_{L-1}+(Lm+Ln+mn)\mathcal{I}_L] \quad \text{(A6)}$$

with

$$\mathcal{I}_L = \frac{1}{2}\int_0^\pi \sin^{2L+1}\theta d\theta \equiv \frac{L!2^L}{(2L+1)!!}\,. \quad \text{(A7)}$$

Particularly simple are the expressions for the upper bound when only the $m = 0, n = 0$ matrix elements are retained, namely $f(r)$ is taken as a constant,

$$\delta E_L = \frac{\hbar^2}{2\mu}\frac{2\langle r^{2L-2}\rangle}{\langle r^{2L}\rangle}L(L+\frac{1}{2})\,, \quad \text{(A8)}$$

which recalls the naive the rotational model. It is worth mentioning the difference between this bound for angular excitations, Eq. (A8) and the bound obtained for radial excitations, Eq. (26), which is manifested specifically in the denominator.

In Table A are given the values obtained for these upper bounds, after solving the generalized eigenvalue problem, and are quite close to the DMC excitation energies displayed in Table II. As in the case of radial excitations, the sum rules have been calculated by means of mixed matrix elements, so that they are not strictly variational.

[1] W. Schöllkopf and J.P. Toennies, Science **266**, 1345 (1994).
[2] W. Schöllkopf and J.P. Toennies, J. Chem. Phys. **104**, 1155 (1996).
[3] O. Kornilov and J.P. Toennies (private communication).
[4] R. Guardiola and J. Navarro, Phys. Rev. Lett. **89**, 193401 (2002).
[5] R. Guardiola and J. Navarro, Few-Body Syst. Suppl. **14**, 223 (2003).
[6] R. Guardiola and J. Navarro, Phys. Rev. A **68**, 055201 (2003).
[7] D. Bressanini, M. Zavaglia, M. Mella and G. Morosi, J. Chem. Phys. **112**, 717 (2000).
[8] D. Bressanini, G. Morosi, L. Bertini, M. Mella, Few-Body Syst. **31**, 199 (2002).
[9] D. Bressanini and G. Morosi, Phys. Rev. Lett. **90**, 133401 (2003).
[10] M. Barranco, M. Pi, S.M. Gatica, E.S. Hernández and J. Navarro, Phys. Rev. B **56**, 8997 (1997).
[11] L.W. Bruch, W. Schöllkopf and J.P. Toennies, J. Chem. Phys. **117**, 1544 (2002).
[12] J. Navarro, M. Barranco, M. Pi, and A. Poves, Phys. Rev. A **69**, in press (2004).
[13] R.A. Aziz, F.R. McCourt and C.C.K. Wong, Mol. Phys. **61**, 1487 (1987).
[14] R.A. Aziz and M.J. Slaman, Jour. Chem. Phys. **94**, 8047 (1991).
[15] K.T. Tang, J.P. Toennies and C.L. Yiu, Phys. Rev. Lett. **74**, 1546 (1995).
[16] F. Dalfovo, Z. Phys. D **14**, 263 (1989).
[17] A. Belič, F. Dalfovo, S. Fantoni and S. Stringari, Phys. Rev. B **49**, 15253 (1994).
[18] E. Krotscheck and R. Zillich, J. Chem. Phys. **115**, 10161 (2001).
[19] J. Lekner, Philos. Mag. **22**, 669 (1970).
[20] R. Guardiola, M. Portesi and J. Navarro, Phys. Rev. B **60**, 6288 (1999).
[21] R. Guardiola and J. Navarro, Phys. Rev. Lett **84**, 1144 (2000).
[22] R. Guardiola, Phys. Rev. B **62**, 3416 (2000).
[23] R. Guardiola, J. Navarro and M. Portesi, Phys. Rev. B **63**, 224519 (2001).
[24] S.A. Chin and E. Krotscheck, Phys. Rev. Lett. **65**, 2658 (1990).
[25] S.A. Chin and E. Krotscheck, Phys. Rev. B **45**, 852 (1992).
[26] M.V. Rama Krisna and K.B. Waley, J. Chem. Phys. **93**, 6738 (1990).

[27] P.J. Reynolds, D.M. Ceperley, B.J. Alder and W.A. Lester Jr., J. Chem. Phys. **77**, 5593 (1982).
[28] J.W. Moskowitz, K.E. Schmidt, M.A. Lee and H.M. Kalos, J. Chem. Phys. **77**, 349 (1982).
[29] J. Vrbik and S.M. Rothstein, J. Comput. Phys. **63**, 130 (1986).
[30] Siu A. Chin, Phys. Rev. A **42**, 6991 (1990).
[31] D.M. Ceperley, in *Recent Progress in Many-Body theories*, edited by J.G. Zabolitzky, M. de Llano, M. Fortes and J.W. Clark, Lect. Not. Phys. **142**, 262 (Springer Verlag, Berlin 1981)